J Mater Sci: Mater Med (2011) 22:1489–1499
DOI 10.1007/s10856-011-4329-0

Enhanced osteoblast and osteoclast responses to a thin film sputtered hydroxyapatite coating

J. Hao · S. Kuroda · K. Ohya · S. Bartakova · H. Aoki · S. Kasugai

Received: 19 November 2010 / Accepted: 27 April 2011 / Published online: 13 May 2011

Abstract A sputtering technique followed by a low temperature hydrothermal treatment has been demonstrated to produce a dense-and-bioactive hydroxyapatite thin film coating. The purpose of the present study was to investigate osteoblast and osteoclast responses to the hydroxyapatite coated plates and titanium plates with similar roughness. Rat bone marrow stromal cells were cultured on these plates to induce osteoblasts. The cells showed a significantly enhanced proliferation on the hydroxyapatite surface, accompanied by increase of osteoblastic phenotypes. The co-cultured osteoclasts exhibited the significantly different cell number and morphology between the hydroxyapatite and the titanium surfaces. A series of osteoclast marker genes were more stimulated on the hydroxyapatite and thirty two percent of the hydroxyapatite surface area could be resorbed by osteoclasts. The thin film sputtered hydroxyapatite could provide a favorable surface for both osteoblast and osteoclast formation and their function, indicating its good osteoconductivity and biodegradability.

J. Hao · S. Kuroda (✉) · S. Kasugai
Section of Oral Implantology and Regenerative Dental Medicine, Tokyo Medical and Dental University, 1-5-45 Yushima, Bunkyo-ku, Tokyo 113-8510, Japan
e-mail: skuroda.mfc@tmd.ac.jp

J. Hao · S. Kasugai
Global Center of Excellence (GCOE), Tokyo Medical and Dental University, Tokyo, Japan

K. Ohya
Section of Pharmacology, Tokyo Medical and Dental University, Tokyo, Japan

S. Bartakova
Department of Prosthodontics, Masaryk University, Brno, Czech Republic

H. Aoki
International Apatite Institute Co, Tokyo, Japan

1 Introduction

Hydroxyapatite (HA), $Ca_{10}(PO_4)_6(OH)_2$, is a well-known bioceramic material for medical application because of its close similarity to the chemical and mineral components of teeth and bones. It has been used to provide bioactive coatings for orthopedic and dental implants [1]. As early as 1960s, the concept of biological fixation of load-bearing implants using HA coatings was proposed as an alternative to cemented fixation. It has been reported that HA coating could provide an excellent long-term success rate in a minimum 10 years follow-up study [2]. Furthermore, the HA coating degradation caused by osteoclastic resorption is considered to be the result of the similar function taking part in the bone remodeling as seen in any other part of the skeleton [3].

A number of methods have been developed to deposit HA coating including plasma spraying, Sol–Gel, pulsed laser deposition, ion-beam method and sputtering. Currently plasma spraying is the major commercially available technique for HA coating due to the high reproducibility and economic efficiency of the process [4, 5]. However, problems cited with the plasma sprayed HA coating include variation in bond strength between the coatings and metallic substrate, non-uniformity in coating density, poor adhesion between the coating and substrates, microcracks on the coating surface and poor resistance to delamination due to the coating process [4, 6]. Thereafter, as an alternative to the plasma spray method, a radio frequency magnetron sputtering technique has been

investigated [7]. The sputtering technique has advantages of depositing thin coatings (0.5–3 μm) with strong adhesion, compact microstructure and controlled elemental composition [8]. However, it has been reported that it is necessary to find an optimal heat treatment to inhibit the dissolution properties of the coating by crystallizing the film [9]. The conventional high temperature (≥600°C) heat treatment may result in the appearance of cracks in the coating because of the difference in the thermal expansion coefficient of Ca–P and metal substrate [7]. For this reason, it is necessary to crystallize the HA film at low temperature. Ozeki et al. reported a hydrothermal technique at as low as 110°C to crystallize sputtered amorphous HA film, and the film-to-substrate adhesion strength increased by over twofold. In vivo pullout tests, a 1.6 times higher bone-bonding strength was achieved by the hydrothermal technique than by the plasma spray method [10]. After the hydrothermal treatment, a surface morphology of needle-like HA crystal was observed by scanning electron microscopy. In addition, the proliferation and alkaline phosphatase (ALP) activity of MC3T3-E1 can be greatly improved by the hydrothermal treatment [11].

Bone is a dynamic tissue, and the long-term maintenance of osseointegration of implant requires a continuous remodeling of the bone-implant interface. Osteoclasts may play an important role in the initial period after implant placement or prepare the implant surface for the bone-forming activity of the osteoblasts [12]. Several investigators have examined the ability of osteoclasts to resorb various forms of calcium phosphate. Gomi et al. reported that osteoclasts form and are capable of resorbing sintered HA and that the rugosity of the HA increases the formation and resorptive activity of the osteoclasts [13]. In contrast, rabbit osteoclasts were found to resorb bone and sintered carbonate apatite but not sintered hydroxyapatite [14]. Those contradictory results might be due to the different sources of the osteoclasts and preparation of calcium phosphates as to crystal structure, grain size and surface roughness [12]. So far, there is no report regarding the osteoclast response to sputtered HA surface.

In the present study, the rat bone marrow stromal cell culture system was used to induce osteoblasts and a co-culture system of primary mouse calvarial osteoblasts and bone marrow cells was performed to entice osteoclast differentiation. And then both osteoblast and osteoclast formation and their function on the surface of the sputtered HA coating were compared to those on rough titanium surface by examining cell proliferation, gene expression and cellular morphological organization. Furthermore, HA coating degradation was also evaluated. The main aim of the present study was to investigate whether the sputtered HA coating would behave in more favorable a manner than non-coated surface-modified titanium substrates.

2 Materials and methods

2.1 Preparation of sputtered HA film on titanium plates

Commercially available grade 2 pure titanium plates ($20 \times 20 \times 1$ mm^3) were used as substrates. Titanium plates coated with or without sputtered HA were manufactured with similar surface roughness. Briefly, all the titanium plates were sandblasted by fluorapatite crystal and then subjected to an acid etching treatment. RF magnetron sputtering was carried out on half of these plates using an SPF-410H (ANELVA Corp.) chamber to produce a HA film with an average thickness of 1.1 μm. Subsequently, a hydrothermal treatment was performed at a temperature of 120°C in an electrolyte solution containing calcium and phosphate ions for 20 h. The composition of the solution was described in detail in the previous study [10]. All samples were sterilized in an autoclave at 121°C for 28 min and packed in polypropylene bags separately. Surface observation and elemental analysis were carried out using scanning electron microscopy (SEM) (JSM-5310LV, JOEL, Tokyo, Japan) and energy dispersive X-ray spectroscopy (EDS) (EMAX-7000, Horiba Ltd., Kyoto). The X-ray diffractometry pattern (XRD) was identified by RINT1400 (Rigaku Corp., Japan) using a CuKα radiation source operating at 50 kV and 100 mA excitation current. The surface roughness (Ra) was determined using a surface measurement tester (SURFCOM 130A).

2.2 Osteoblastic cell culture

Rat bone marrow cells were prepared according to the method of Maniatopoulos et al. [15]. Briefly, rat bone marrow cells isolated from the femora of 5 week-old male Wistar rats were cultured on these plates placed in 6-well culture dishes at a cell density of 10^6 cells/cm^2, maintained in α-MEM with 10% fetal bovine serum at 37°C in a humidified atmosphere consisting of 95% air and 5% CO_2. After 24 h, the medium was removed and changed to fresh one supplemented with osteogenic reagents (50 μg/ml ascorbic acid, 10 mM β-glycerophosphate, 10 nM dexamethasone). The culture medium was changed every 2 days.

2.3 Cell attachment and proliferation

After 24 and 72 h incubation, the culture medium was removed and the wells were washed three times with phosphate buffered saline (PBS) to eliminate unattached cells. The adherent bone marrow stromal cells were fixed and stained using fluorescent dyes, DAPI (molecular probes, Invitrogen, USA), and observed under a fluorescence microscope (Biozero BZ-8000, Keyence). In

addition, the proliferative activity of the cells was measured by BrdU incorporation during DNA synthesis. At day 2 of culture, BrdU reagent with the final concentration of 10 μM (Roche Applied Science, Mannheim, Germany) was added to the culture wells and incubated for 10 h at 37°C. After the labeling process, the cells were fixed and incubated with anti-BrdU-peroxidase working solution for 90 min. After washing, substrate solution (tetramethylbenzidine) followed by stop solution was added until color development was sufficient for photometric detection. Absorbance at 450 nm was measured using Wallace 1420 ARVOsx multi-label counter.

2.4 Measurement of DNA amount and ALP activity

Cells were washed with PBS, scraped, lysed by 0.1% Triton X100 (Sigma, St. Louis, MO, USA), and sonicated to destroy cell membranes. After centrifugation at 15,000 rpm for 10 min at 4°C, 200 μl of the supernatant was extracted from each sample and assayed for ALP activity and DNA content measurements. To determine DNA content, 100 μl of the prepared supernatant of each sample was mixed with 100 μl of 1 μg/ml Hoechst 33342 dye in the wells of a 96-well plate and processed with a fluorescent DNA quantification kit (Bio-Rad Laboratories, Hercules, CA, USA). The samples were then measured with the Wallace 1420 ARVOsx multi-label counter at excitation and emission wavelengths of 365 and 460 nm, respectively. Subsequently, to assess the quantitative and kinetic determination of ALP activity, 50 μl of the supernatant of each sample was added to 100 μl working solution (*p*-nitrophenyl phosphate solution) in the wells of another 96-well plate. The reaction was measured with the multi-label counter at a wavelength of 405 nm. ALP activity was normalized by total DNA amount of each sample.

2.5 Mineralization assay

The mineralization capability of cultured osteoblasts was examined at days 7 and 21. The cells were fixed with methanol and stained with Alizarin Red. The area of mineralized nodules of each sample was measured using a computer image analyzer (Image J, National Institute of Health, USA). To eliminate non-specific binding of Alizarin Red Stain, nodules bigger than 0.2 mm^2 were calculated. The result is represented as percentages of Alizarin Red positive area over total culture area.

2.6 Osteoclastic cell culture

Osteoclasts generated by a co-culture system [16] were also cultured on these titanium plates inserted in 6-well culture dishes. Briefly, osteoblast (3×10^5 cells/well) obtained by sequential collagenase digestion of newborn mouse calvariae and bone marrow cells (3×10^6 cells/well) obtained from femora and tibiae of 6 week-old male ICR mice were co-cultured in the normal medium (α-MEM, 10% fetal bovine serum) supplemented with 10^{-8} M 1,25-$(OH)_2$-vitamin D_3 and 10^{-6} M prostaglandin E_2. For osteoclast morphology and function assays, the co-culture was also performed on ivory dentine slices and polystyrene culture wells as control.

2.7 Osteoclast number and morphology

After 4, 5 and 7 days co-culture, cells were fixed with 3.7% formaldehyde in PBS for 10 min and washed three times with PBS and permeabilized with 0.1% Triton X-100 in PBS for 5 min. The cells were rinsed three times with PBS and treated with 1% bovine serum albumin for 10 min. Cells were stained using fluorescent dyes, 5 units/ml Alexa 488 phalloidin (actin green color, Molecular Probes, Invitrogen, USA) and 300 nM DAPI (nuclei blue color, Molecular Probes, Invitrogen, USA). Subsequently, tartrate-resistant acid phosphatase (TRAP) staining was also performed. In brief, cells were rinsed with ethanol–acetone solution (50:50, v/v) for 1 min, and stained with TRAP solution for 10 min at room temperature. To prepare TRAP solution, 5 mg of naphthol AS-MX phosphate (Sigma, USA) was diluted in 0.5 ml of *N*,*N*-dimethylformamide (Wako, Japan) and this solution was combined with 30 mg of fast red violet LB salt (Sigma, USA) and 50 ml of 0.1 M sodium acetate buffer (pH 5.9) containing 50 mM sodium tartrate. TRAP positive cells with three or more nuclei were considered as osteoclasts. TRAP positive cells and cellular structures such as actin and multi-nuclei were visualized using a fluorescence microscope (Biozero BZ-8000, Keyence). The osteoclast number, area, perimeter and Feret's diameter were quantified by an image analyzer (Image J, National Institute of Health, USA).

2.8 HA coating degradation

At osteoclast culture day 7, the HA samples were soaked in 1 M ammonia, and the cells were removed by sonicating for 1 min. To analyze the HA coating degradation, element distribution of the HA coating was performed by energy dispersive X-ray mapping. The HA coated samples immersed in the same culture medium for 7 days were used as control. The coating degradation area was calculated by Image J.

2.9 RNA isolation and real-time quantitative RT-PCR

Cells in both culture systems were lysed in TRIzol Reagent (Invitrogen, USA) and total RNA was precipitated in

isopropanol. First-strand cDNA was reverse-transcribed from total RNA with SuperScript™ IIIFirst-Strand Synthesis System for RT-PCR (Invitrogen, USA). The expression levels of osteoblast or osteoclast related genes were determined using the real-time quantitative reverse transcription-polymerase chain reaction (RT-PCR). SYBR Green-based real-time PCR analysis was carried out with the ABI Prism 7,300 Sequence Detection System (Applied Biosystems, Foster City, CA, USA). Expression levels were determined using the relative threshold cycle (C_T) method as described by the manufacturer of the detection system. Expression levels were stated in terms of fold increase or decrease relative to that of Ti group at the first time point. This was calculated for each gene by evaluating the expression $2^{-\Delta\Delta CT}$, where $\Delta\Delta$CT is the result of subtracting $[C_{T\ gene}-C_{T\ GAPDH}]_{(Ti\ calibrator)}$ from $[C_{Tgene}-C_{TGAPDH}]_{(HA\ group)}$. The primers used are shown in Table 1.

2.10 Statistical analysis

All experiments were performed in duplicate, and results were calculated as mean ± SD. Statistical analysis was performed by the statistic software 11.5 SPSS for Windows. ANOVA with Scheffe test was used for comparing the significance among groups at each time point. *t*-Test was used to determine the differences between the HA and Ti groups if data were available at only one time point. *P* values of less than 0.05 were considered to be statistically significant.

3 Results

3.1 The observations and characterizations of sputtered HA coating

Fig. 1a showed the XRD pattern of sputtered HA coating. The dotted lines and solid lines indicated the peaks of Ti and crystallized HA, respectively. EDS analysis confirmed the purity of the Ti (Fig. 1b) and the sputtered HA coating (Fig. 1c). The Ra values of the Ti and sputtered Ha coating were 1.25 ± 0.26 and 1.13 ± 0.39 μm, respectively. The Ca/P molar ratio was 1.70 ± 0.13 (Table 2).

Table 1 Real time RT-PCR primers

Gene	Sequence	Base pair	Sequence reference
Mouse GAPDH	(F) 5′ -CTCCCACTCTTCCACCTTCG-3′	99	NM008084
	(R) 5′-TTGCTGTAGCCGTATTCATT-3′		
Mouse TRAP	(F) 5′-TACCTGTGTGGACATGACC-3′	151	BC029644
	(R) 5′-CAGATCCATAGTGAAACCGC-3′		
Mouse v-ATPase	(F) 5′-TCCAACACAGCCTCCTACTT-3′	161	AB022322
	(R) 5′-ACAGCAAAGGCAGCAAAC-3′		
Mouse CTR	(F) 5′-TCAGGAACCACGGAATCCTC-3′	101	NM007588
	(R) 5′-ACATTCAAGCGGATGCGTCT-3′		
Mouse CathepsinK	(F) 5′-TGTATAACGCCACGGCAAA-3′	195	X94444
	(R) 5′-GGTTCACATTATCACGGTCACA-3′		
Mouse MMP-9	(F) 5′-TCCAGTACCAAGACAAAG-3′	183	X72795
	(R) 5′-TTGCACTGCACGGTTGAA-3′		
Mouse RANKL	(F) 5′-ACCAGCATCAAAATCCCAAG-3′	203	AB008426
	(R) 5′-TTGAAAGCCCCAAAGTACGT-3′		
Rat GAPDH	(F) 5′-AACTCCCATTCTTCCACCTT-3′	200	M17701.1
	(R) 5′-TCTCGTTCTCTCTCCGGGA-3′		
Rat TGF-β1	(F) 5′-CAACAATTCCTGGCGTTACC-3′	200	NM_021578.2
	(R) 5′-TTAGTTACCCTAGTCAGGGT-3′		
Rat ALP	(F) 5′-GTCACAGCCAGTCCCTCAAC-3′	202	NM_013059.1
	(R) 5′-GCTGAGGGGACAAACCTTAT-3′		
Rat Col1	(F) 5′-TTGACCCTAACCAAGGATGC-3′	197	NM_053356.1
	(R) 5′-TTATGTTGCGTCTTCCCCAC-3′		
Rat Runx2	(F) 5′-GCCAGGTTCAACGATCTGAG-3′	201	NM_053470.1
	(R) 5′-CAAACAAGAGACTGGCGGAG-3′		
Rat osteocalcin	(F) 5′-AGCTCAACCCCAATTGTGAC-3′	190	M11777
	(R) 5′-TTTCATACCTGCCGTGTCGA-3′		

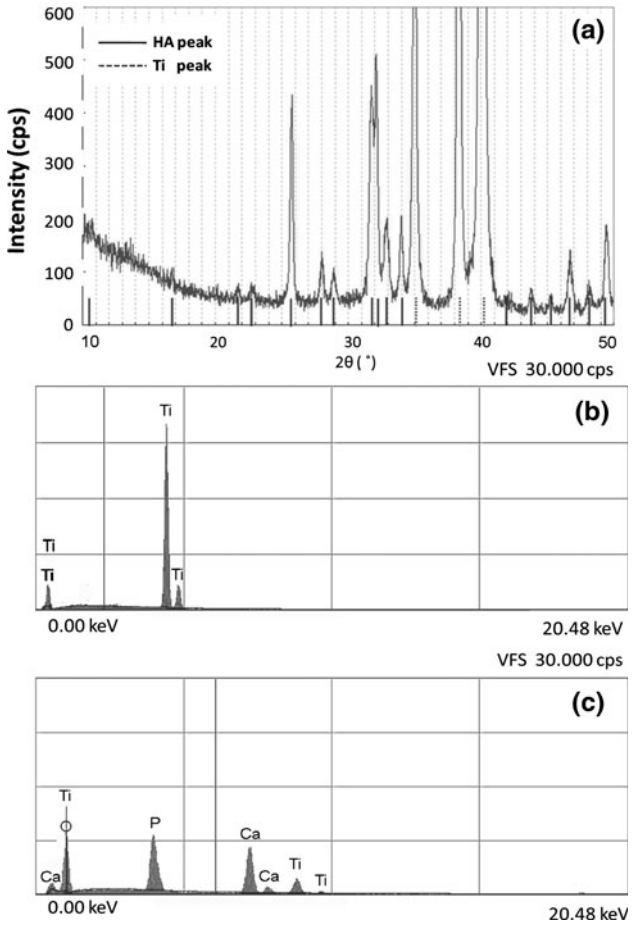

Fig. 1 X-ray diffractometry (XRD) pattern of the sputtered HA film (**a**). Energy dispersive X-ray spectroscopy (EDS) spectrum of the Ti plate (**b**) and the sputtered HA coated Ti plate (**c**)

3.2 Enhanced attachment and proliferation of bone marrow stromal cells on sputtered HA surface

Cell density was consistently greater on the sputtered HA surfaces (Fig. 2b, d) than that on Ti surfaces (Fig. 2a, c) at days 1 and 3**.** The proliferation determined by BrdU incorporation also showed a significantly higher level on the sputtered HA surface compared with Ti surfaces, confirming increased cell proliferation (Fig. 2e).

3.3 Enhanced osteoblastic phenotypes on sputtered HA surface

ALP activity was measured on days 3, 7 and 14. In both groups, ALP activity increased time dependently. In detail, ALP activity was showing the same level on both surfaces at day 3; however, cells on sputtered HA at days 7 and 14 accelerated ALP activity at a significant higher level compared with those of the Ti group (Fig. 3a).

In addition, the area of mineralized nodule detected by Alizarin Red stain was also greater on HA surface. At day 7, the HA group showed a 4.3 fold increase in nodule formation compared to the Ti group ($P < 0.01$). Until day 21, the HA group still exhibited a higher level of nodule formation than the Ti group ($P < 0.05$) (Fig. 3b). Real-time PCR demonstrated mRNA expressions of osteoblastic marker genes of interest as fold changes to the control level. Rat mRNA expression levels of ALP and TGF-β were significantly increased on HA surface by day 7 ($P < 0.05$). However, the other genes including osteocalcin, collagen type I and runx2 showed significant increases only at day 14 ($P < 0.05$) (Fig. 3c–g).

Table 2 Surface roughness and Ca/P ratio. ($n = 3$)

Sample	Ra (μm)	Ca/P
Ti	1.25 ± 0.26	
HA	1.13 ± 0.39	1.70 ± 0.13

3.4 Osteoclast formation and morphometry

TRAP positive cells were observed in all experimental groups as early as day 4 of the co-culture. The fluorescence microscopy images of actin structures of these multinucleated cells overlapped with the TRAP staining (Fig. 4a–h).

Osteoclasts could form on several substrates and then exhibit different actin structures. Phalloidin fluorescence staining showed that the actin ring sizes were increasing from day 4 to day 7. Moreover, the actin ring structure on the sputtered HA surface was consistently showing smaller size compared to that on the Ti surface and the polystyrene culture well, but almost the equal size to that on dentine slice (control > Ti > HA ≈ dentine) (Fig. 5a–c). Osteoclasts on Ti and polystyrene surface were exhibiting typical podosome belts with loose actin network by small actin dots, also called actin cloud (Fig. 4e, g). In contrast, the osteoclasts on both HA and dentine were able to acquire a sealing zone, represented by a dense band of actin (Fig. 4a, c).

As shown in Fig. 5d, the number of osteoclasts on the dentine or HA was larger than those on Ti and the control surfaces throughout the culture period ($P < 0.01$). Significant difference of TRAP positive cell number between the dentin and the HA groups was found only at day 4 ($P < 0.01$) but not at days 5 and 7.

3.5 Osteoclast function and HA coating degradation

To further confirm the functionality of the osteoclasts, the mRNA levels of a series of their growth and differentiation markers including receptor activator of nuclear factor kappa B ligand (RANKL), osteoprotegerin (OPG), TRAP,

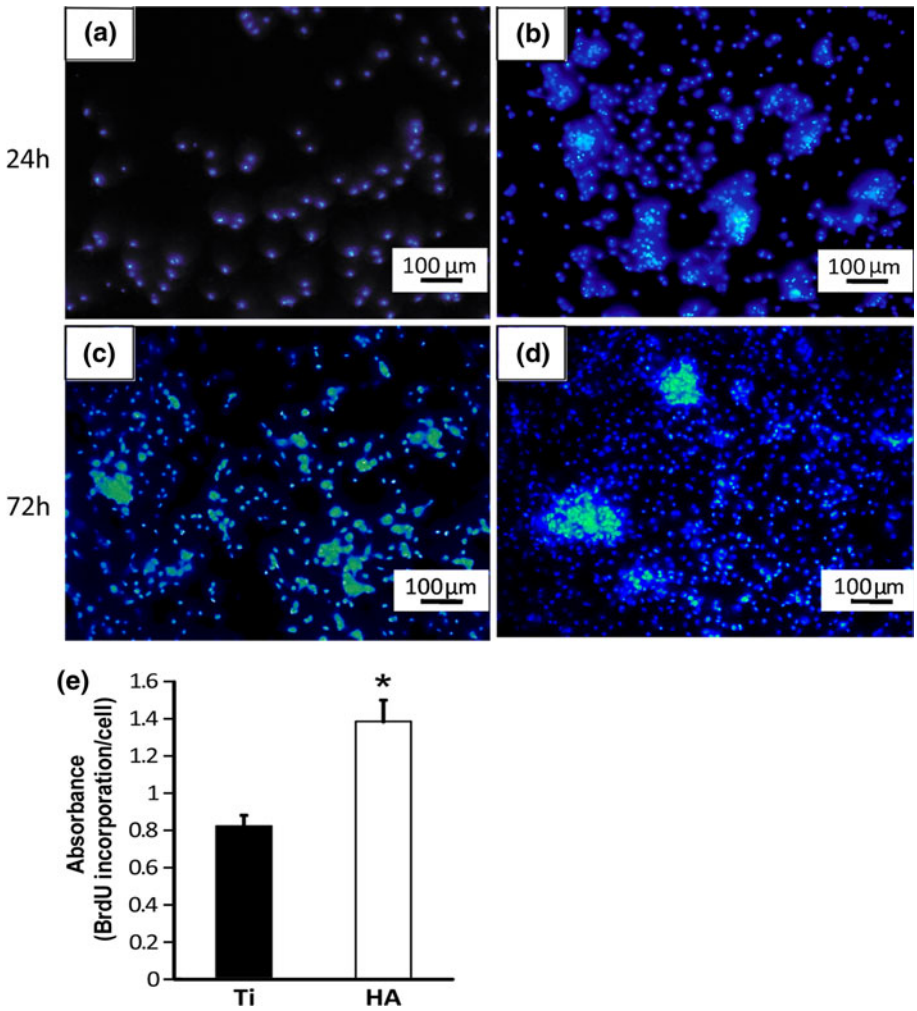

Fig. 2 Initial behavior of bone marrow stromal cells on the Ti and the HA surfaces. DAPI staining of bone marrow cells attached to the Ti (**a**, **c**) and the HA (**b**, **d**) after 24 h (**a**, **b**) and 72 h (**c**, **d**) incubation. The cell proliferation was determined by BrdU incorporation and the absorbance measurement at 450 nm (**e**). And each column represents values as the mean ± SD ($n = 6$). *Statistically different between HA and Ti groups ($P < 0.05$)

vacuolar-type H-ATPase (v-ATPase), calcitonin receptor (CTR), cathepsin K, and MMP-9 were analyzed by quantitative real-time RT-PCR. V-ATPase and the ratio of RANKL/OPG mRNA expression were significantly increased on HA than on Ti at day 5 and so were TRAP and CTR transcription at day 7. However, no differences could be observed in terms of Cathepsin K and MMP-9 expression (Fig. 6a–h).

After 7 days of culture, cells were removed from the samples and the coating degradation was analyzed by energy dispersive X-ray mapping. The elemental distribution of calcium, phosphorus and titanium was shown in Fig. 7. The regions with HA degradation were indicated with arrows in Fig. 7a–d, where, Ca and P were completely absent. In addition, these regions were rich in Ti which indicated the degradation of the HA coating and the titanium substrate exposure. However, in the control group, no coating degradation was observed after soaking in the same culture medium for 7 days. Ca and P were homogeneously distributed throughout the HA coating, and Ti could be hardly detected (Fig. 7e–h). These results suggested that the coating degradation were mediated by osteoclastic functional resorption but not HA chemical dissolution. The osteoclastic degradation occurred in 32.3 ± 3.5% of the sputtered HA coating.

4 Discussion

In this study, a rat bone marrow stromal cell culture was performed to evaluate the osteoblast response on the HA coated titanium. One advantage of cell culture systems is that it can focus on a part of the physiological condition, wherein interaction among the cells and signal molecules can be clarified. Since the implant materials directly contact bone marrow cells after implantation, it is advantageous to use a culture system to investigate implant materials as substrates for the cells [17]. The cell density was consistently greater on the sputtered HA surface than the Ti surface on days 1 and 3 of culture, wherein, by day 3, the cells had appeared to reach confluence on the HA surface but not on the Ti surface. Notably, this increment of

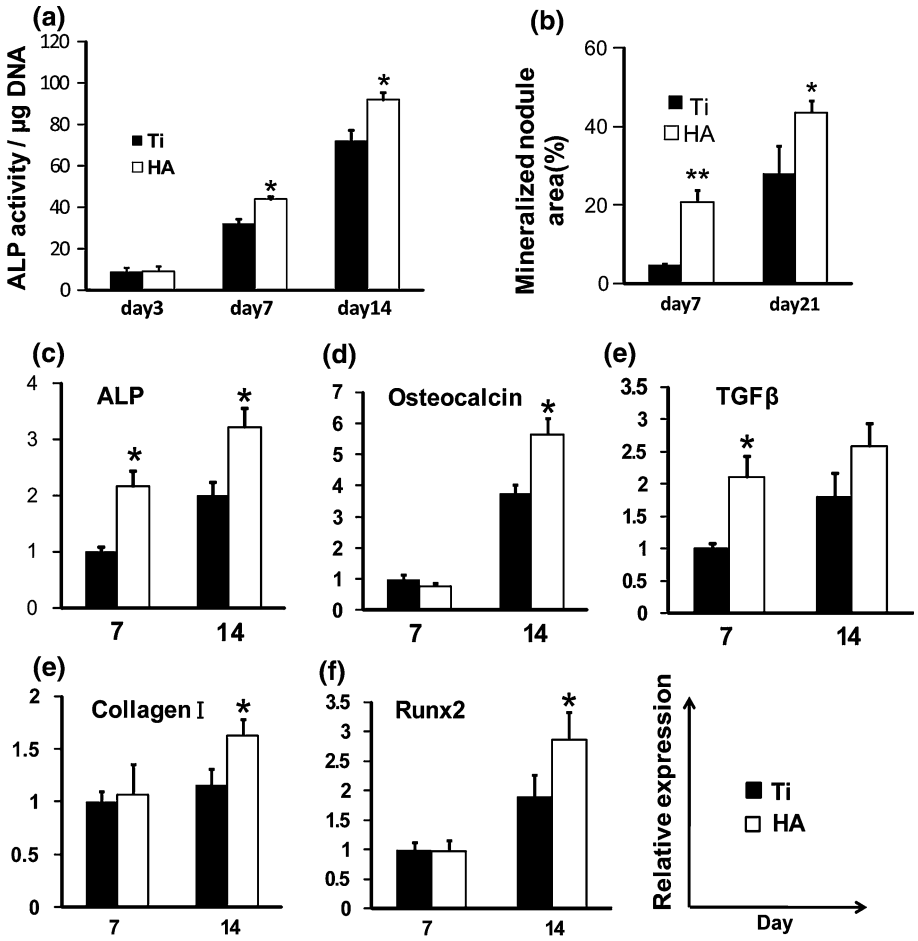

Fig. 3 Enhanced osteoblastic phenotypes on the sputtered HA surface. A quantitative analysis of ALP activity was performed by normalizing total ALP amount by total DNA content (**a**). The Alizarin *red* positive staining is represented as percentages of the total culture area (**b**). mRNA expression levels of osteoblast-related genes (**c**–**g**), where x-axis represent days of culture, and y-axis represent expression levels relative to Ti group of the first time point. Data are shown as the mean ± SD ($n = 6$). Statistically different between HA and Ti groups (*$P < 0.05$, **$P < 0.01$)

the cell number might be reflected by emphasized BrdU incorporation on the HA at day 2 (68% higher than on the Ti surface). These current results indicated that the sputtered HA surface could significantly enhance the bone marrow stromal cells compared with Ti surface. Since the surface of the sputtered HA and the titanium was manufactured with similar roughness, the enhanced proliferation on the HA may have been due to the difference in the chemical composition of the coating.

ALP expression is associated with osteoblastic differentiation and the level of ALP activity indicates the stage of osteoblastic differentiation. In the present study, the ALP activity was significantly elevated on the sputtered HA surface than on the Ti surface from day 7. This is in line with the previous study that hydrothermally treated sputtered HA film could promote the ALP activity of MC3T3-E1 osteoblast-like cells after 96 h culture [11]. The significantly increased gene expression levels of collagen I, runx2, osteocalcin and ALP on the sputtered HA surface further supported the results. Furthermore, the mineralized nodule deposition on HA was 1.8 times as extensive as that on Ti ($P < 0.05$), indicating that the sputtered HA surface provided a favorable surface for bone marrow cell adhesion, proliferation and osteoblast differentiation.

Osteoclast is the principal cell responsible for the resorption of bone during bone remodeling. The organization of the actin cytoskeleton plays an important role in the resorption function of osteoclasts. Depending on the substratum upon which the osteoclasts spread, actin presents flat podosomes or sealing zone. It has been reported that when osteoclasts adhere on plastic or glass, podosomes are arranged at the osteoclast periphery as a characteristic belt. If adhering to a mineralized matrix, osteoclasts polarize and exhibit a typical sealing zone which delineates the ruffled border, a site of active membrane traffic and transport, where protons and proteases are secreted in order to dissolve minerals by acidification and degrade extracellular matrix proteins. A large surface area (>3,000 μm^2) corresponded to spreading of non-resorbing osteoclasts without sealing zone. In contrast, cell surfaces between 1,700 and 2,000 μm^2 corresponded to actively resorbing osteoclasts exhibiting a sealing zone [18]. In the present study, the osteoclasts on the HA surface always showed smaller size compared with those on the Ti and the polystyrene culture wells, but close to that on the dentine. The

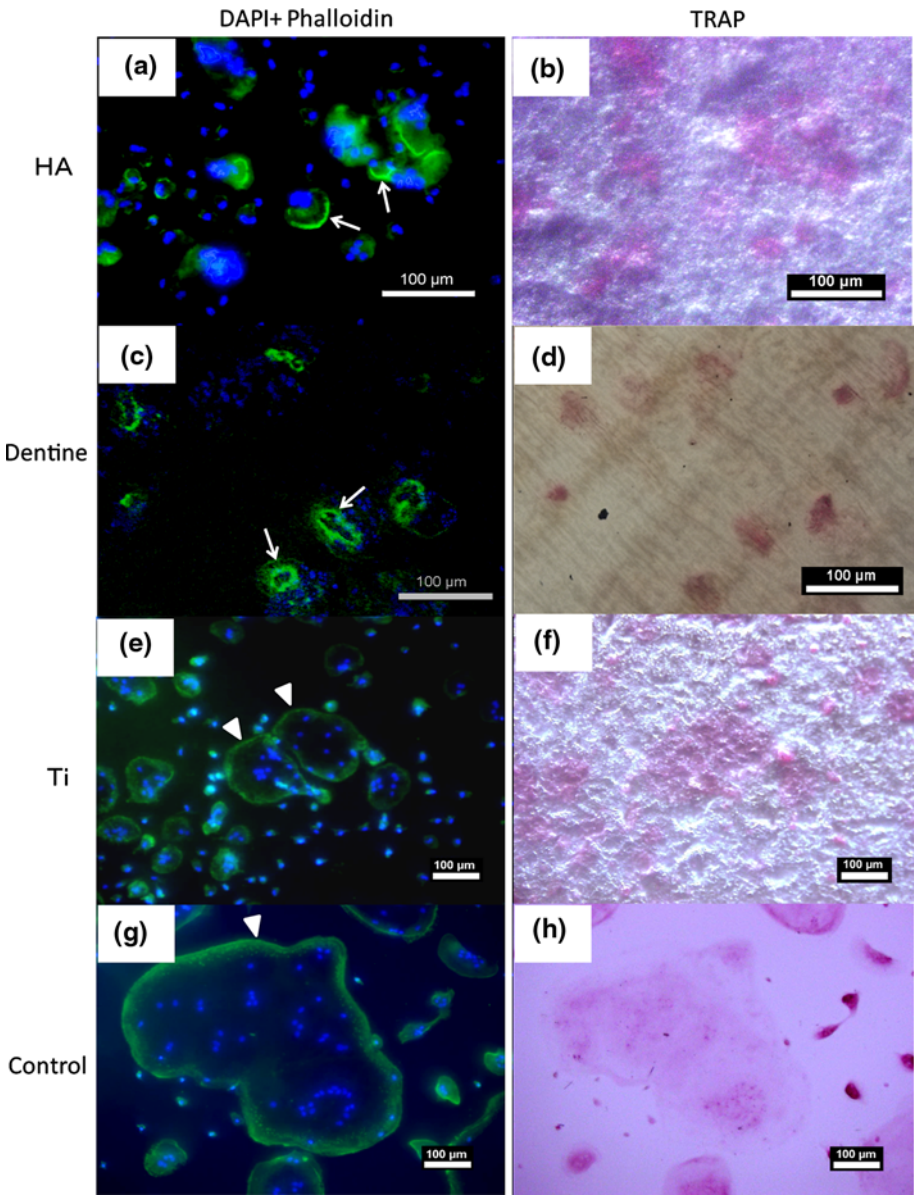

Fig. 4 Osteoclast formation and cytoskeletal arrangement. Micrographs show osteoclastic differentiation on HA (**a**, **b**), dentine (**c**, **d**), Ti (**e**, **f**) and control polystyrene culture wells (**g**, **h**) at co-culture day 5. Cells were stained with DAPI for nuclei (*blue*) and phalloidin for actin filaments (*green*) (**a**, **c**, **e**, **g**) and with TRAP (**b**, **d**, **f**, **h**). Sealing zones, represented by actin rings were indicated by *arrows*, and prodosome belts were indicated by *arrow heads*

typical podosome belt structure represented as actin dots was found at the periphery of the osteoclast on the Ti and the polystyrene culture wells. However, on both the HA coating and dentine surfaces, a much denser but smaller actin ring structure-sealing zone was shown. These results were also consistent with the previous finding that the size of each actin dot within the sealing zone on a mineralized matrix is four times larger than that on plastic or glass surface [18]. From these results it could be suggested that osteoclast formed on the sputtered HA surface could apico-basal polarize, and exhibit a typical sealing zone, inside of which the active resorption takes place. The osteoclasts formed on the sputtered HA surface could have a similar morphology and behavior to those on the dentine. And the element distribution of the HA coating was further analyzed by EDS mapping, confirming that 32.3 ± 3.5% of the sputtered HA coating area degradation was mediated by osteoclastic resorption.

During the differentiation of the progenitor cells to osteoclasts, a series of osteoclast markers were analyzed. TRAP is highly expressed in osteoclasts, and the secretion of TRAP by osteoclasts represents the rate of resorptive activity [19]. CTR is regarded as the best late-stage differentiation marker for osteoclasts, which distinguishes them from macrophage polykaryons [20]. During osteoclastic resorption, hard tissues are demineralized by v-ATPase [21] and collagens are subsequently degraded by cathepsin K [22] and MMP-9 [23]. In the present study, TRAP and CTR were expressed at significantly higher levels on HA than on Ti at day 7. v-ATPase expression level was increased on HA at day 5. However, no differences could be observed in terms of Cathepsin K and

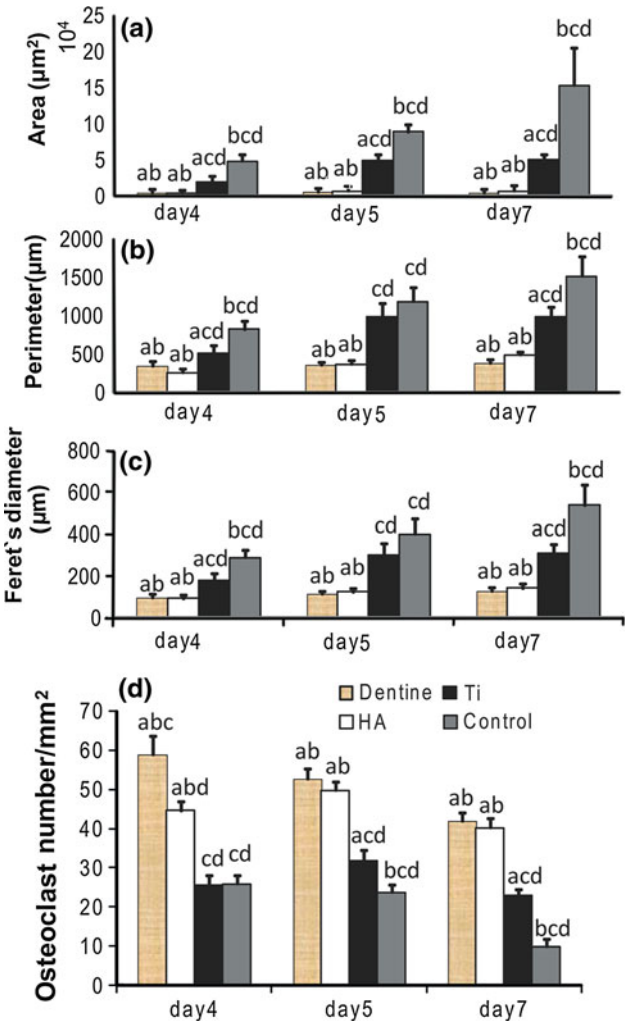

Fig. 5 Osteoclast morphometry. The area (**a**), perimeter (**b**) and Feret's diameter (**c**) (Feret's diameter is the longest distance between any two points along the osteoclast surface) were quantified using an image analyzer (Image J). TRAP positive cells with three or more nuclei were counted (**d**). Each value is represented as the mean ± SD ($n = 6$). Statistically different ($P < 0.01$): **a** compared with control, **b** compared with Ti, **c** compared with HA and **d** compared with dentine

MMP-9 mRNA expression. These results suggest that the sputtered HA surface stimulated osteoclast formation and function by controlling the mRNA transcription that regulates osteoclast.

We also examined the expressions of RANKL and its decoy receptor OPG. The RANKL/OPG ratio plays a crucial role in coordinating the sequence of osteoclast differentiation during the bone remodeling cycle [24]. In the present study, OPG mRNA level was slightly increased on HA than on Ti although the difference was not significant and the level of RANKL mRNA on HA was significantly elevated at day 5, which resulted in an apparent increase in RANKL/OPG ratio favorable for osteoclast formation. A few studies have addressed the effect of implant microtopography on osteoclast formation and activity. Lossdörfer S et al. cultured MG63 cells on titanium disks with different surface roughness, and found that OPG mRNA levels increased on rougher surfaces while RANKL expression was independent of surface microtopography [25]. We observed a higher RANKL/OPG ratio on the sputtered HA than on Ti in the present study. It is probably due to the difference of chemical composition between HA and Ti. Our results for the first time suggested that the sputtered HA surface might stimulate osteoclast formation by up-regulation of RANKL expression from osteoblasts in the co- culture system.

Another explanation of our findings is that HA has the ability to adsorb and release proteins because it has multiple potential protein binding sites and a larger specific surface area compared to other calcium phosphates. The HA film has an adsorption site at the *a*-plane area (Ca^{2+}) and at the *c*-plane area (PO_4^-, OH^-), which can attract acidic proteins with negative sites (COO^-) and basic proteins with positive sites (NH_2^+), respectively [26]. The previous study has reported that the surface area of the sputtered HA film was increased by the hydrothermal treatment, owing to the growth of HA crystals in the *c*-axis direction [27]. The adsorption amount of proteins is proportionate to the surface area of HA, and the release rate of proteins depends on HA resorption [28]. Additionally, osteoclast adhesion and migration are regulated by $\alpha_v\beta_3$ integrin which binds to a variety of extracellular matrix proteins including vitronectin, osteopontin and bone sialoprotein [29], and osteoprogenitor cells and osteoblasts also express a wide panel of integrins, which regulate osteoblast function and mineralization [30, 31]. In the present study, the sputtered HA may promote the osteoblast and osteoclast formation and function through the integrin mediated signaling pathway as a result of recruitment of extracellular matrix proteins onto the coating. Further studies are needed to elucidate the mechanism in detail from this point of view.

Recently, several studies suggested that osteoclast, besides the resorptive activity, may have an anabolic effect on bone formation. Zhao et al. reported that the cell surface molecule ephrinB2 present on the osteoclasts mediated anabolic signals to the osteoblasts [32]. In further support of the role of osteoclast in bone formation, Karsdal et al. showed that ostoeclasts secreted non-bone derived factors which induce preosteoblasts to form bone-like nodules [33]. Thereby, these findings indicate the importance of the presence of osteoclasts for induction of bone formation. Better understanding of how osteoclasts respond to different implant surfaces may help contribute to the development of implants that improve osseointergration.

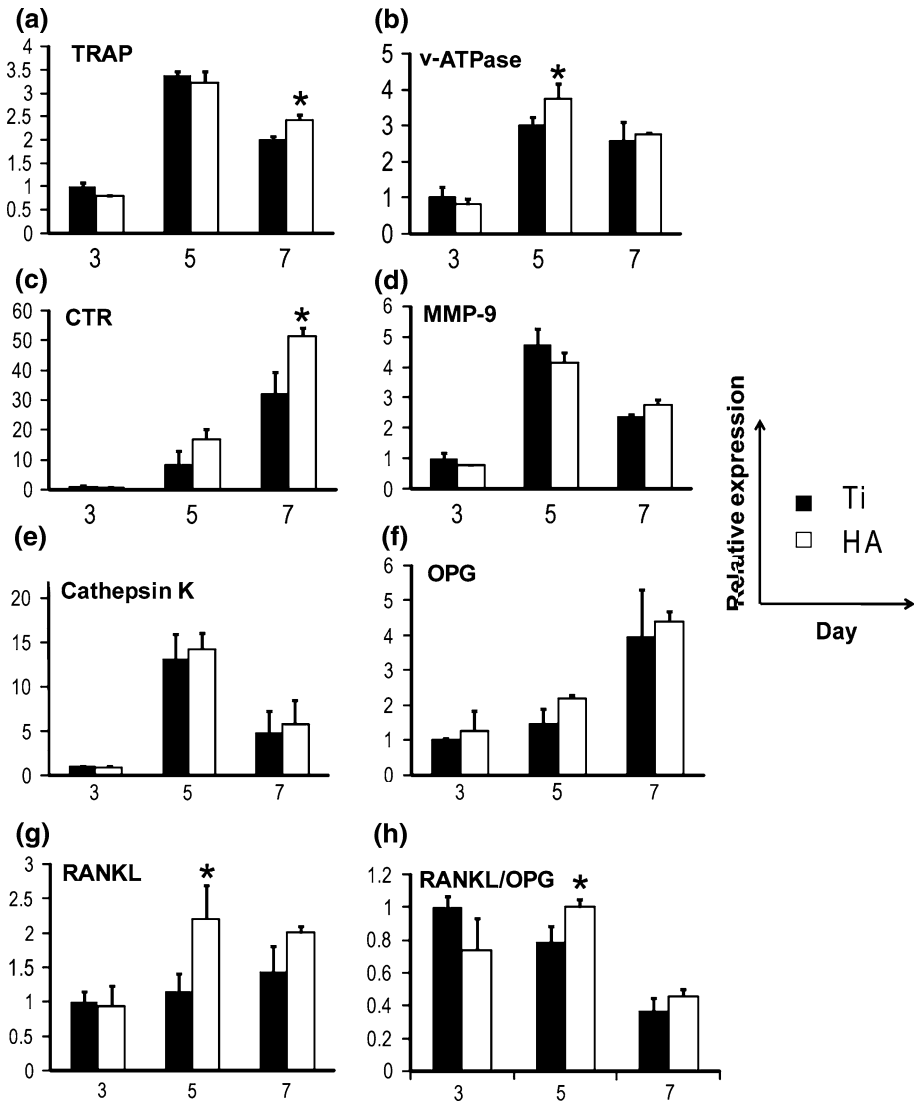

Fig. 6 mRNA expression levels of osteoclast related genes. X-axes represent days of culture, and y-axes represent expression levels relative to Ti group of the first time point. Data are shown as the mean ± SD ($n = 6$). *Statistically different between HA and Ti groups ($P < 0.05$)

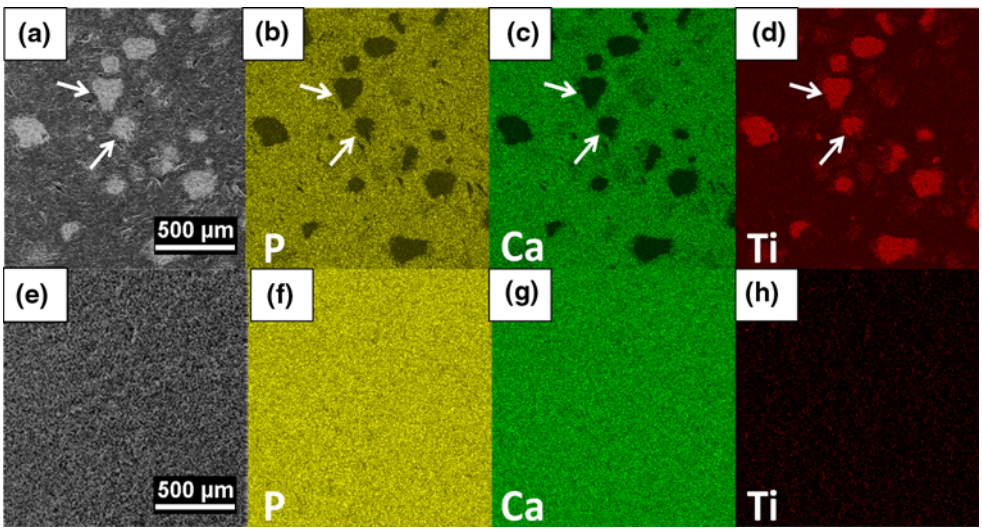

Fig. 7 SEM micrographs of HA coating (**a**, **e**) and corresponding X-ray elemental maps for P in *yellow* (**b**, **f**), Ca in *green* (**c**, **g**) and Ti in *red* (**d**, **h**). Osteoclast culture was performed on the HA coated Ti plates for 7 days and the resorption areas were indicated by *arrows* (**a**–**d**). The HA coated Ti plates with no cells were soaked in the same culture medium for 7 days as control (**e**–**h**)

5 Conclusion

In conclusion, our study demonstrated that the thin film sputtered HA coating provides a more favorable surface for bone marrow stromal cell attachment, proliferation and osteoblastic differentiation and function than the surface-modified titanium. The sputtered HA coating also supported osteoclast formation and function which indicated its favorable biodegradability. Therefore, the sputtered HA coating may have an outstanding potential to be used as a drug delivery system in orthopedic and dental applications for more rapid and complete bone-implant integration.

Acknowledgments The authors thank Dr. H. Shimokawa, Dr. S. Ichinose and Mr. Y. Hashimoto for technical assistance and helpful advice. This study was supported by the Global Center of Excellence (GCOE) Program, International Research Center for Molecular Science in Tooth and Bone Disease's, Tokyo Medical and Dental University, Tokyo, Japan.

References

1. Lacefield WR. Hydroxyapatite coatings. Ann N Y Acad Sci. 1988;523:72–80.
2. Bidar R, Kouyoumdjian P, Munini E, Asencio G. Long-term results of the ABG-1 hydroxyapatite coated total hip arthroplasty: analysis of 111 cases with a minimum follow-up of 10 years. Rev Chir Orthop Traumatol. 2009;95(8):579–87.
3. Thomas KA. Hydroxyapatite coatings. Orthopedics. 1994;17(3): 267–78.
4. Narayanan R, Seshadri SK, Kwon TY, Kim KH. Calcium phosphate-based coatings on titanium and its alloys. J Biomed Mater Res B. 2008;85(1):279–99.
5. Ong JL, Chan DC. Hydroxyapatite and their use as coatings in dental implants: a review. Crit Rev Biomed Eng. 2000;28(5–6): 667–707.
6. Zhu X, Son DW, Ong JL, Kim K. Characterization of hydrothermally treated anodic oxides containing Ca and P on titanium. J Mater Sci Mater Med. 2003;14(7):629–34.
7. van Dijk K, Schaeken HG, Wolke JG, Jansen JA. Influence of annealing temperature on RF magnetron sputtered calcium phosphate coatings. Biomaterials. 1996;17(4):405–10.
8. Massaro C, Baker MA, Cosentino F, Ramires PA, Klose S, Milella E. Surface and biological evaluation of hydroxyapatite-based coatings on titanium deposited by different techniques. J Biomed Mater Res. 2001;58(6):651–7.
9. Yang Y, Kim KH, Ong JL. A review on calcium phosphate coatings produced using a sputtering process—an alternative to plasma spraying. Biomaterials. 2005;26(3):327–37.
10. Ozeki K, Mishima A, Yuhta T, Fukui Y, Aoki H. Bone bonding strength of sputtered hydroxyapatite films subjected to a low temperature hydrothermal treatment. Biomed Mater Eng. 2003; 13(4):451–63.
11. Ozeki K, Aoki H, Fukui Y. Dissolution behavior and in vitro evaluation of sputtered hydroxyapatite films subject to a low temperature hydrothermal treatment. J Biomed Mater Res A. 2006;76(3):605–13.
12. Minkin C, Marinho VC. Role of the osteoclast at the bone-implant interface. Adv Dent Res. 1999;13:49–56.
13. Gomi K, Lowenberg B, Shapiro G, Davies JE. Resorption of sintered synthetic hydroxyapatite by osteoclasts in vitro. Biomaterials. 1993;14(2):91–6.
14. Doi Y, Shibutani T, Moriwaki Y, Kajimoto T, Iwayama Y. Sintered carbonate apatites as bioresorbable bone substitutes. J Biomed Mater Res. 1998;39(4):603–10.
15. Maniatopoulos C, Sodek J, Melcher AH. Bone formation in vitro by stromal cells obtained from bone marrow of young adult rats. Cell Tissue Res. 1988;254(2):317–30.
16. van't Hof RJ. Osteoclast formation in the mouse coculture assay. In: Helfrich MH, Ralston SH, editors. Bone research protocols. Totowa: Humana Press; 2003. p. 145–52.
17. Ozawa S, Kasugai S. Evaluation of implant materials (hydroxyapatite, glass-ceramics, titanium) in rat bone marrow stromal cell culture. Biomaterials. 1996;17(1):23–9.
18. Saltel F, Destaing O, Bard F, Eichert D, Jurdic P. Apatite-mediated actin dynamics in resorbing osteoclasts. Mol Biol Cell. 2004;15(12):5231–41.
19. Kirstein B. Secretion of tartrate resistant acid phosphatase by osteoclasts correlates with resorptive behavior. J Cell Biochem. 2006;98(5):1085–94.
20. Roodman GD. Advances in bone biology: the osteoclast. Endocr Rev. 1996;17(4):308–32.
21. Sasaki T, Hong MH, Udagawa N, Moriyama Y. Expression of vacuolar H(+)-ATPase in osteoclasts and its role in resorption. Cell Tissue Res. 1994;278(2):265–71.
22. Saftig P, Hunziker E, Wehmeyer O, Jones S, Boyde A, Rommerskirch W, et al. Impaired osteoclastic bone resorption leads to osteopetrosis in cathepsin-K-deficient mice. Proc Natl Acad Sci USA. 1998;95(23):13453–8.
23. Tezuka K, Nemoto K, Tezuka Y, Sato T, Ikeda Y, Kobori M, et al. Identification of matrix metalloproteinase 9 in rabbit osteoclasts. J Biol Chem. 1994;269(21):15006–9.
24. Gori F, Hofbauer LC, Dunstan CR, Spelsberg TC, Khosla S, Riggs BL. The expression of osteoprotegerin and RANK ligand and the support of osteoclast formation by stromal-osteoblast lineage cells is developmentally regulated. Endocrinology. 2000;141(12): 4768–76.
25. Lossdörfer S, Schwartz Z, Wang L, Lohmann CH, Turner JD, Wieland M, et al. Microrough implant surface topographies increase osteogenesis by reducing osteoclast formation and activity. J Biomed Mater Res A. 2004;70(3):361–9.
26. Aoki H. Medical applications of hydroxyapatite. Tokyo, St. Louis: Ishiyaku EuroAmerica Inc.; 1994.
27. Ozeki K, Aoki H, Fukui Y. Effect of pH on crystallization of sputtered hydroxyapatite film under hydrothermal conditions at low temperature. J Mater Sci. 2005;40(11):2837–42.
28. Matsumoto T, Okazaki M, Inoue M, Yamaguchi S, Kusunose T, Toyonaga T, et al. Hydroxyapatite particles as a controlled release carrier of protein. Biomaterials. 2004;25(17):3807–12.
29. Nakamura I, Duong IT, Rodan SB, Rodan GA. Involvement of alpha(v)beta3 integrins in osteoclast function. J Bone Miner Metab. 2007;25(6):337–44.
30. Keselowsky BG, Collard DM, García AJ. Integrin binding specificity regulates biomaterial surface chemistry effects on cell differentiation. Proc Natl Acad Sci USA. 2005;102(17):5953–7.
31. Schneider GB, Zaharias R, Stanford C. Osteoblast integrin adhesion and signaling regulate mineralization. J Dent Res. 2001; 80(6):1540–4.
32. Zhao C, Irie N, Takada Y, Shimoda K, Miyamoto T, Nishiwaki T, et al. Bidirectional ephrinB2-EphB4 signaling controls bone homeostasis. Cell Metab. 2006;4(2):111–21.
33. Karsdal MA, Neutzsky-Wulff AV, Dziegiel MH, Christiansen C, Henriksen K. Osteoclasts secrete non-bone derived signals that induce bone formation. Biochem Biophys Res Commun. 2008; 366(2):483–8.